

# Effect of Cathodic Hydrogen Evolution on the Coercivity and Thermal Stability of Sintered NdFeB Magnets

Nan Haiyang, Zhu Liqun, Liu Huicong, Li Weiping

Beihang University, Beijing 100191, China

**Abstract:** The effect of cathodic hydrogen evolution on coercivity and thermal stability was investigated in sintered NdFeB magnets. The magnetic properties, phase structure and morphology were studied by SQUID-VSM, DSC, XRD, TEM and SEM. After cathodic hydrogen evolution, the  $H_{cj}$  decreases from 1034.8 kA m<sup>-1</sup> to 963.16 kA m<sup>-1</sup>. The temperature coefficient  $\alpha$  declines from  $-0.253\% \cdot ^\circ\text{C}^{-1}$  to  $-0.3229\% \cdot ^\circ\text{C}^{-1}$ , and the  $\beta$  declines from  $-0.7518\% \cdot ^\circ\text{C}^{-1}$  to  $-0.7738\% \cdot ^\circ\text{C}^{-1}$ . A mechanism was proposed to explain the results. In the process of cathodic hydrogen evolution, some of the generated hydrogen atoms react with the Nd<sub>2</sub>Fe<sub>14</sub>B phase and Nd-rich phase, forming Nd<sub>2</sub>Fe<sub>14</sub>BH<sub>x</sub> and NdH<sub>x</sub>, respectively. The formation of NdH<sub>x</sub> causes a volume expansion, which results in intergranular cracks and stress. X-ray diffraction and morphology characterization confirms the presence of these defects. These defects would significantly promote the nucleation of reverse magnetic domains, and further decline the coercivity and thermal stability of magnets.

**Key words:** NdFeB; coercivity; thermal stability; hydrogen

Sintered NdFeB magnets are widely used in electronic industry, wind power generation and electric vehicle, due to their excellent magnetic properties<sup>[1,2]</sup>. The magnets have poor corrosion resistance<sup>[3,4]</sup>. Surface treatment is necessary to improve the corrosion resistance. Electroplating Ni, Zn and Ni/Cu/Ni coatings or electrophoresis of epoxy coating are the most commonly used surface treatments in industry<sup>[5,6]</sup>. However, it has been noticed that these surface treatments declined the magnetic properties<sup>[7-11]</sup>. In the electroplating or electrophoresis processes, cathodic hydrogen evolution is the main side reaction and inevitable, while the composition, microstructure and magnetic properties of NdFeB magnets are sensitive and vulnerable to hydrogen. It is reasonable to relate the declined magnetic properties with cathodic hydrogen evolution. Coercivity and thermal stability are important magnetic properties for the application of magnets, especially at high temperature. So it is very significant to clarify how cathodic hydrogen evolution affects the coercivity and thermal stability.

The magnets are composed of matrix Nd<sub>2</sub>Fe<sub>14</sub>B phase and intergranular Nd-rich phase. The coercivity and thermal

stability are in close relation with the composition and microstructure of magnets. Additions including Ce<sup>[12]</sup>, Ho<sub>63.4</sub>Fe<sub>36.6</sub><sup>[13]</sup>, DyH<sub>x</sub><sup>[14]</sup>, Y<sub>72</sub>Co<sub>28</sub><sup>[15]</sup>, Dy<sub>82.3</sub>Co<sub>17.7</sub><sup>[16]</sup> and Zr<sup>[17]</sup> etc. were used to enhance the coercivity and thermal stability by composition and microstructure optimization. While the local stress near the grain boundary<sup>[18]</sup>, cracks in the magnets<sup>[19]</sup> and lattice misfit of N-rich phase with Nd<sub>2</sub>Fe<sub>14</sub>B phase<sup>[20]</sup> all could decline the coercivity. Thus, identifying the relations among cathodic hydrogen evolution, composition and microstructure is particularly important.

In the present study, we investigated how cathodic hydrogen evolution declined the coercivity and thermal stability. A mechanism was proposed to explain this phenomenon. This knowledge would also provide a chance to avoid the coercivity and thermal stability decline or regain them.

## 1 Experiment

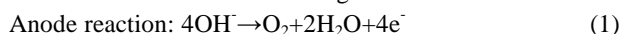
The commercial sintered NdFeB magnets (Nd<sub>15.1</sub>Tb<sub>0.6</sub>Fe<sub>77.4</sub>B<sub>6.9</sub>) were used in the investigation. Magnets were polished with SiC abrasive papers (of grades in the range of 600~2000), ultrasonically cleaned in alcohol and

Received date: December 20, 2016

Corresponding author: Nan Haiyang, Candidate for Ph. D., School of Material Science and Engineering, Beihang University, Beijing 100191, P. R. China, Tel: 0086-10-82317113, E-mail: nanhy@buaa.edu.cn

Copyright © 2017, Northwest Institute for Nonferrous Metal Research. Published by Elsevier BV. All rights reserved.

then dried in air. The cathodic hydrogen evolution was performed in 3.5 wt% NaCl solution with a DC power supply (KAE-1201) at room temperature. The 3.5 wt% NaCl solution was used to simulate the aqueous salt solution in electroplating and electrophoresis. Magnets and Pt plate were used as cathode and anode, respectively. Hydrogen was generated at the NdFeB magnets surface with cathodic current density of 0.2, 0.5 and 1 A/dm<sup>2</sup> for 30 min. In actual electroplating or electrophoresis process, the cathodic current density usually varied from a few tenths of amperes per square decimeter to several amperes per square decimeter. The cathodic current density was also bigger in the edges and corners of cathode due to tip effect. The deposition time varied from tens of minutes to hours. So these cathodic current density and time were chosen in the experiment. The electrode reaction was as following<sup>[21]</sup>:



Magnetic properties were measured using an SQUID-VSM magnetic measurement device with a maximum magnetic field of 7 T at 300 and 373 K. The Curie temperature was tested by differential scanning calorimetry (DSC, NETZSCH) at a heating rate of 10 °C/min. Phase analysis was examined by X-ray diffraction (XRD, Rigaku, Japan) with Cu K $\alpha$

radiation. Transmission electron microscopy was carried out by FEI Tecnai G2 F20 operated at 200 kV. The surface morphologies were characterized by field emission scanning electron microscopy (FESEM, Apollo 300).

## 2 Results and Discussion

Fig.1 shows the remanence ( $B_r$ ), coercivity ( $H_{c_j}$ ) and maximum energy product ( $(BH)_{\text{max}}$ ) of the original and treated NdFeB magnets. The  $H_{c_j}$  declines obviously after cathodic hydrogen evolution. It declines from 1034.8 to 963.16 kA m<sup>-1</sup> at 300 K, and from 469.64 kA m<sup>-1</sup> to 421.88 kA m<sup>-1</sup> at 373 K. The  $B_r$  and  $(BH)_{\text{max}}$  also declines significantly. However, when the cathodic current density increases to 1 A/dm<sup>2</sup>, the magnetic properties recover partly. This might be due to the shedding of the most hydrogenated surface grains, which would be discussed later.

Fig.2 shows the differential scanning calorimetry (DSC) curves of the original and treated NdFeB magnets. It indicates the Curie temperature ( $T_C$ ) is affected by cathodic hydrogen evolution. The  $T_C$  increases by about 2 °C from the original 310 °C after cathodic hydrogen evolution. The increased  $T_C$  results from the volume expansion, which is induced by hydrogen entering crystal lattice of magnets<sup>[22]</sup>.

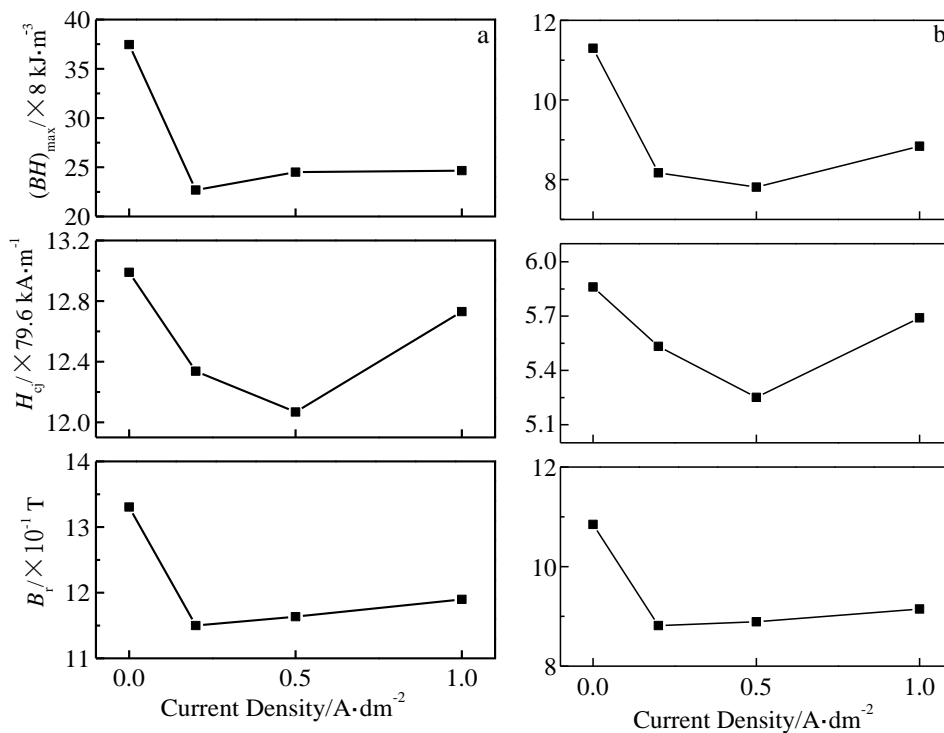


Fig.1 Remanence ( $B_r$ ), coercivity ( $H_{c_j}$ ) and maximum energy product ( $(BH)_{\text{max}}$ ) of NdFeB magnets treated by cathodic hydrogen evolution with different current density for 30 min tested at 300 K (a) and 373 K (b)

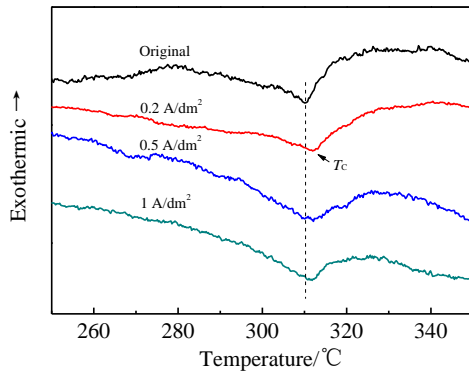


Fig.2 DSC curves of original and treated NdFeB magnets by cathodic hydrogen evolution for 30 min

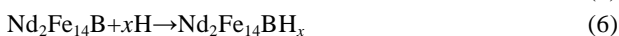
The temperature coefficients of  $B_r$  ( $\alpha$ ) and  $H_{cj}$  ( $\beta$ ) of magnets from 300 K to 373 K are shown in Fig.3. They reflect the thermal stability of magnets, which are calculated from the following formulas:

$$\alpha = \frac{B_{rT} - B_{rT_0}}{B_{rT_0}(T - T_0)} \times 100\% \quad (3)$$

$$\beta = \frac{H_T - H_{T_0}}{H_{T_0}(T - T_0)} \times 100\% \quad (4)$$

where  $\alpha$  and  $\beta$  are the temperature coefficients of  $B_r$  ( $\alpha$ ) and  $H_{cj}$  ( $\beta$ ) at temperature range from  $T_0$  to  $T$ , respectively. The  $\alpha$  declines from  $-0.253\% \cdot ^\circ\text{C}^{-1}$  to  $-0.3229\% \cdot ^\circ\text{C}^{-1}$ , and the  $\beta$  declines from  $-0.7518\% \cdot ^\circ\text{C}^{-1}$  to  $-0.7738\% \cdot ^\circ\text{C}^{-1}$  after cathodic hydrogen evolution. It is shown the cathodic hydrogen evolution reduces the thermal stability of magnets.

The coercivity and thermal stability are in close relation with the composition and microstructure of magnets. To investigate the effect of cathodic hydrogen evolution on the composition and microstructure of magnets, XRD, TEM and SEM were employed in the study. The diffraction patterns of the original and treated NdFeB magnets are shown in Fig.4. The diffraction peaks are characteristic peaks of  $\text{Nd}_2\text{Fe}_{14}\text{B}$  phase (PDF 36-1296) and Nd-rich phase (PDF 07-0090)<sup>[23]</sup>. No new diffraction peaks appear in the patterns of treated magnets. However, all the diffraction peaks shift relatively toward smaller diffraction angles. This reveals that cathodic hydrogen evolution expands the lattice parameters of the  $\text{Nd}_2\text{Fe}_{14}\text{B}$  phase and Nd-rich phase. It is due to that parts of the generated hydrogen atoms react with the  $\text{Nd}_2\text{Fe}_{14}\text{B}$  phase and Nd-rich phase, forming  $\text{Nd}_2\text{Fe}_{14}\text{BH}_x$  and  $\text{NdH}_x$ , respectively<sup>[24,25]</sup>. The reaction is as following<sup>[21,26]</sup>:



TEM images of the original and treated NdFeB magnets

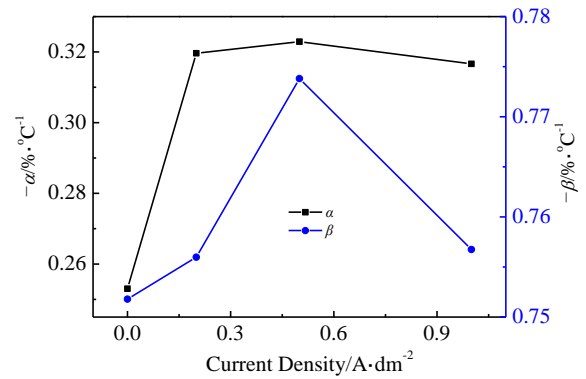


Fig.3 Temperature coefficients (from 300 K to 373 K) of remanence ( $\alpha$ ) and coercivity ( $\beta$ ) of the NdFeB magnets treated by cathodic hydrogen evolution for 30 min

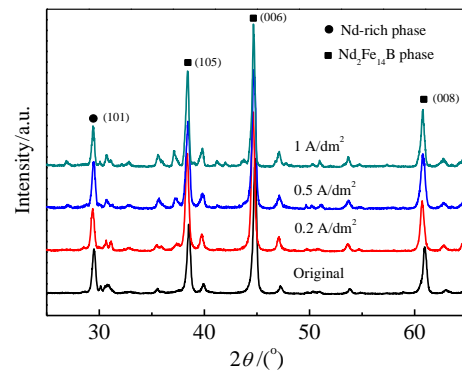


Fig.4 XRD patterns of original and treated NdFeB magnets by cathodic hydrogen evolution for 30 min

are shown in Fig.5. The results of FETEM test are consistent with that of XRD. As shown in the images and SAED pattern, the crystal structure of tetragonal  $\text{Nd}_2\text{Fe}_{14}\text{B}$  phase and hexagonal close packed (hcp) Nd-rich phase do not change after cathodic hydrogen evolution. Limited by accuracy, the expansion of lattice parameters could not be discerned directly in the image.

The surface morphologies of the original and treated NdFeB magnets are shown in Fig.6. The original magnets are compact. After  $0.2 \text{ A/dm}^2$  cathodic hydrogen evolution for 30 min, some intergranular cracks and bulged matrix grains appear, as shown in Fig.6a and 6b.

It is due to the absorption of hydrogen by the  $\text{Nd}_2\text{Fe}_{14}\text{B}$  phase and Nd-rich phase, as mentioned in the XRD analysis. The formation of  $\text{NdH}_x$  causes a volume expansion of the grain boundary<sup>[27,28]</sup>, which results in intergranular cracks and stress. With the adding of current density, the volume

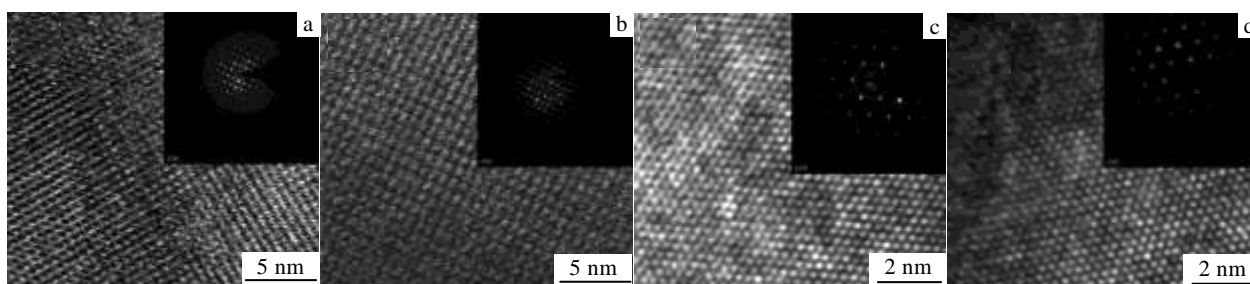


Fig.5 TEM images and selected area electron diffraction patterns of original NdFeB magnets (a, c) and the magnets treated by cathodic hydrogen evolution with  $0.5 \text{ A/dm}^2$  for 30 min (b, d): (a, b)  $\text{Nd}_2\text{Fe}_{14}\text{B}$  phase and (c, d) Nd-rich phase

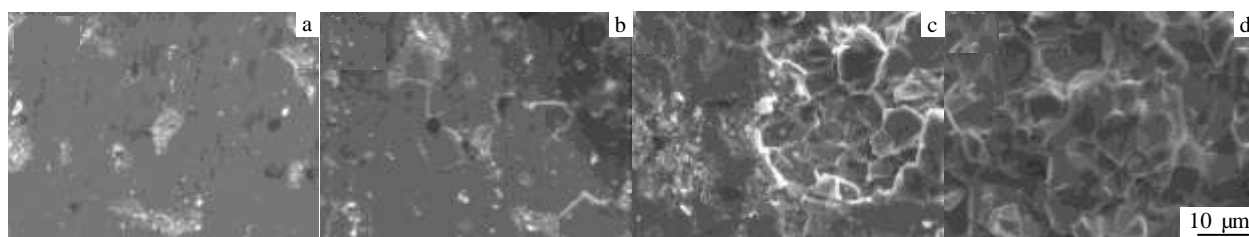


Fig.6 Surface morphologies of original NdFeB magnets (a) and the magnets treated by cathodic hydrogen evolution for 30 min: (b)  $0.2 \text{ A/dm}^2$ , (c)  $0.5 \text{ A/dm}^2$ , and (d)  $1 \text{ A/dm}^2$

expansion also increases. Parts of grains shred from magnets surface after  $0.5 \text{ A/dm}^2$  cathodic hydrogen evolution. And almost all surface grains shred after  $1 \text{ A/dm}^2$  cathodic hydrogen evolution. The intergranular cracks are obvious in the images. The shedding of the most hydrogenated surface grains might partly recover the declined magnetic properties, as mentioned previously.

Cathodic hydrogen evolution induces some changes of composition and microstructure in the magnets, including the interstitial hydrogen, intergranular cracks and stress. These changes would promote the nucleation of reverse magnetic domains, which further declines the coercivity and thermal stability of the magnets. In NdFeB magnets, the coercivity is determined by the activation energy of reverse magnetic domains nucleation. The phenomenological equation is used<sup>[19]</sup>:

$$H_{cj} = aH_a - N_{eff}M_s \quad (7)$$

where  $H_a$  is the anisotropy field,  $a$  is structure factor,  $M_s$  is the spontaneous magnetization, and  $N_{eff}$  is the effective demagnetization factor. The interstitial hydrogen would decrease  $H_a$ <sup>[22]</sup>. And the intergranular cracks and stress would increase the  $N_{eff}$ <sup>[19]</sup>. These situations all lead to declined coercivity. At a relatively high temperature, the treated magnets would be more prone to nucleate reverse magnetic domains, which also decreases the thermal stability. To avoid the coercivity and thermal stability of magnets declining, suppressing the cathodic hydrogen evolution in surface

treatments should receive more attention.

### 3 Conclusions

1) Cathodic hydrogen evolution results in declined coercivity and thermal stability of sintered NdFeB magnets. The  $H_{cj}$  decreases from  $1034.8 \text{ kA m}^{-1}$  to  $963.16 \text{ kA m}^{-1}$  at 300 K. The  $\alpha$  declines from  $-0.253\% \cdot \text{C}^{-1}$  to  $-0.3229\% \cdot \text{C}^{-1}$ , and the  $\beta$  declines from  $-0.7518\% \cdot \text{C}^{-1}$  to  $-0.7738\% \cdot \text{C}^{-1}$ . The  $B_r$  and  $(BH)_{max}$  also drops significantly.

2) Cathodic hydrogen evolution expands the lattice parameters of the  $\text{Nd}_2\text{Fe}_{14}\text{B}$  phase and Nd-rich phase, and forms  $\text{Nd}_2\text{Fe}_{14}\text{BH}_x$  and  $\text{NdH}_x$ . The formation of  $\text{NdH}_x$  causes a volume expansion of the grain boundary, which results in intergranular cracks and stress.

3) The interstitial hydrogen, intergranular cracks and stress would promote the nucleation of reverse magnetic domains, which further decreases the coercivity and thermal stability of magnets.

### References

- 1 Zhang Y J, Ma T Y, Liu X L et al. *Journal of Magnetism and Magnetic Materials*[J], 2016, 399: 159
- 2 Wang X L, Zhao L N, Ding K H et al. *Chinese Physics B*[J], 2015, 24(3): 358
- 3 Isotahdon E, Huttunen-Saarivirta E, Heinonen S et al. *Journal of Alloys and Compounds*[J], 2015, 626: 349

- 4 Zhang X, Ma Y T, Zhang B et al. *Corrosion Science*[J], 2014, 87: 156
- 5 Yang H X, Mao S D, Song Z G. *Rare Metal Materials and Engineering*[J], 2011, 40(12): 2241 (in Chinese)
- 6 Li B, Wang C B, Wang X D et al. *Rare Metal Materials and Engineering*[J], 2015, 44(1): 174 (in Chinese)
- 7 Cheng Y Y, Pang X L, Gao K W et al. *Thin Solid Films*[J], 2014, 550: 428
- 8 Li J L, Wang Y X, Wang L P. *Thin Solid Films*[J], 2014, 568: 87
- 9 Mao S D, Xie T T, Zheng B Z et al. *Surface & Coatings Technology*[J], 2012, 207: 149
- 10 Xie T T, Mao S D, Yu C et al. *Vacuum*[J], 2012, 86(10): 1583
- 11 Cheng C W, Man H C, Cheng F T. *IEEE Transactions on Magnetics*[J], 1997, 33(5): 3910
- 12 Pei K, Zhang X, Lin M et al. *Journal of Magnetism and Magnetic Materials*[J], 2016, 398: 96
- 13 Liang L P, Ma T Y, Wu C et al. *Journal of Magnetism and Magnetic Materials*[J], 2016, 397: 139
- 14 Ma T Y, Wang X J, Liu X L et al. *Journal of Physics D: Applied Physics*[J], 2015, 48(21): 215 001
- 15 Ding G F, Guo S, Cai L W et al. *IEEE Transactions on Magnetics*[J], 2015, 51(8): 2 100 504
- 16 Zhang X F, Guo S, Yan C J et al. *Journal of Applied Physics*[J], 2014, 115(17): 17A757
- 17 Liu Z W, Qian D Y, Zhao L Z et al. *Journal of Alloys and Compounds*[J], 2014, 606: 44
- 18 Liu Q Z, Xu F, Wang J et al. *Scripta Materialia*[J], 2013, 68(9): 687
- 19 Akiya T, Sasaki T T, Ohkubo T et al. *Journal of Magnetism and Magnetic Materials*[J], 2013, 342: 4
- 20 Kim T H, Lee S R, Namkung S et al. *Journal of Alloys and Compounds*[J], 2012, 537: 261
- 21 Yang H, Mao S, Song Z. *Materials and Corrosion*[J], 2012, 63(4): 292
- 22 Chang H, Zhang X D, Yang Y C. *Solid State Communications*[J], 2001, 119(6): 403
- 23 Mao S D, Yang H X, Song Z L et al. *Corrosion Science*[J], 2011, 53(5): 1887
- 24 Guo S, Zhou Q Y, Chen R J et al. *Journal of Applied Physics*[J], 2011, 109(7): 07A734
- 25 Tan C L, Bai S X, Zhang H et al. *Journal of Alloys and Compounds*[J], 2004, 368(1-2): 333
- 26 Guo S, Liu Y H, Chen B C et al. *Journal of Applied Physics*[J], 2012, 111(7): 07A740
- 27 Kim A S, Camp F E, Lizzi T. *Journal of Applied Physics*[J], 1996, 79(8): 4840
- 28 Li J J, Li A H, Zhu M G et al. *Journal of Applied Physics*[J], 2011, 109(7): 07A744

## 阴极析氢对钕铁硼磁体矫顽力和热稳定性的影响

南海洋, 朱立群, 刘慧丛, 李卫平  
(北京航空航天大学, 北京 100191)

**摘要:** 研究了由阴极析氢导致的烧结钕铁硼磁体矫顽力和热稳定性下降。使用SQUID-VSM、DSC、XRD、TEM和SEM系统地研究了磁性能, 相结构和形貌的变化。阴极析氢后, 300 K时矫顽力从1034.8 kA m<sup>-1</sup>下降到963.16 kA m<sup>-1</sup>。温度系数 $\alpha$ 从-0.253%·°C<sup>-1</sup>下降到-0.3229%·°C<sup>-1</sup>,  $\beta$ 从-0.7518%·°C<sup>-1</sup>下降到-0.7738%·°C<sup>-1</sup>。其作用机制如下: 在阴极析氢过程中, 部分产生的氢与Nd<sub>2</sub>Fe<sub>14</sub>B相和富钕相反反应, 相应地生成Nd<sub>2</sub>Fe<sub>14</sub>BH<sub>x</sub>和NdH<sub>x</sub>。生成的NdH<sub>x</sub>会体积膨胀, 导致了晶间裂纹和应力。XRD和微观形貌都确认了这些缺陷的存在。这些缺陷促进了反磁化畴的形核, 进而降低了磁体的矫顽力和热稳定性。

**关键词:** 钕铁硼; 矫顽力; 热稳定性; 氢

作者简介: 南海洋, 男, 1986年生, 博士生, 北京航空航天大学材料科学与工程学院, 北京 100191, 电话: 010-82317113, E-mail: nanhy@buaa.edu.cn